Formulation and Optimization of liposomal drug delivery system for Anticancer Therapy

Ms. Rupali D. Bandgar[1] , Dr. Pravin Uttekar[2] Ms. Ankita Barshile[3] Dr. Rakesh Wani[4]

1) Student of M. Pharmacy, Late Lakshimibai Phadtare College of Pharmacy, Kalamb,Walchandnagar.
2) Principal of Late Lakshimibai Phadtare College of Pharmacy,Kalamb,Walchandnagar.
3) Assistant Professor of Late Lakshimibai Phadtare College of Pharmacy, Kalamb,Walchandnagar.
4) Assistant Professor of Late Lakshimibai Phadtare College of Pharmacy, Kalamb,Walchandnagar.

Abstract:

Cancer chemotherapy often suffers from inadequate drug selectivity, systemic toxicity, and adverse effects that limit doses and reduce therapeutic effectiveness. Liposomal drug delivery systems have emerged as promising nanocarriers that can enhance the pharmacokinetics and therapeutic efficacy of anticancer agents through targeted delivery and controlled drug release. This study aimed to develop and optimize methotrexate-loaded liposomes to improve anticancer treatment using the thin-film hydration method and a Box–Behnken experimental design. Liposomes were created using soya lecithin and cholesterol, and the impact of formulation variables on essential quality attributes was assessed. The formulated preparations were analyzed for parameters such as particle size, polydispersity index (PDI), zeta potential, drug concentration, entrapment efficiency, and in vitro drug release. The structural and physicochemical properties of the optimized formulation were assessed using Fourier Transform Infrared (FTIR) spectroscopy, X-ray diffraction (XRD), and Transmission Electron Microscopy (TEM). Statistical optimization techniques were utilized to pinpoint the formulation that exhibited the most favorable physicochemical characteristics and prolonged drug release. The optimized liposomal formulation showcased nanoscale vesicles with a tight particle size distribution, excellent colloidal stability, high drug entrapment efficiency, adequate drug concentration, and sustained release of methotrexate in vitro. FTIR and XRD analyses verified the compatibility between the drug and the formulation components, while TEM observations displayed spherical liposomal vesicles that were uniformly distributed. Stability investigations revealed that the optimized formulation retained its physicochemical

properties throughout the duration of the study. The results indicate that the refined methotrexate-loaded liposomal formulation represents a promising method for targeted delivery of anticancer drugs by improving drug encapsulation, enhancing formulation stability, and enabling controlled release of the drug. This liposomal delivery mechanism holds the potential to increase the therapeutic effectiveness of methotrexate while minimizing systemic toxicity, making it a valuable strategy for the advancement of nanocarrier-based cancer therapies.

Keywords: Liposomes, Methotrexate, Cancer treatment Drug delivery system;.

INTRODUCTION :

Cancer continues to be one of the top causes of death globally and remains a significant public health concern, despite notable progress in diagnosis and treatment. Traditional treatment methods, such as surgery, radiotherapy, and chemotherapy, have improved survival rates for patients; however, their effectiveness is often hindered by issues like non-specific drug distribution, systemic toxicity, low bioavailability, and the emergence of multidrug resistance. Among these therapeutic options, chemotherapy is still fundamental for treating various solid tumors and blood cancers, yet its lack of selectivity frequently leads to severe negative effects on healthy tissues, diminishing therapeutic effectiveness and patient adherence. Nanotechnology-driven drug delivery systems have emerged as innovative solutions to address the shortcomings of standard chemotherapy. These systems enhance the pharmacokinetics of anticancer drugs, boost drug stability, extend systemic circulation, and enable targeted delivery to tumor sites while reducing off-target toxicity. Among different nanocarriers, liposomes have garnered significant interest due to their outstanding biocompatibility, biodegradability, low immunogenic response, and capacity to encapsulate both hydrophilic and hydrophobic therapeutic agents. Liposomes, which are vesicles made from phospholipid bilayers, can safeguard encapsulated drugs from early degradation and ensure controlled drug release. Their preferential accumulation in tumor tissues, facilitated by the enhanced permeability and retention (EPR) effect, further amplifies therapeutic efficacy while minimizing systemic exposure. Methotrexate is a commonly utilized antimetabolite and antifolate chemotherapy drug that is effective in treating a variety of cancers, such as leukemia, lymphoma, breast cancer, osteosarcoma, and cancers of the head and neck. Although it has demonstrated anticancer efficacy, its clinical use is hindered by issues such as low selectivity, rapid distribution throughout the body, toxic effects that depend on dosage, and negative impacts on healthy tissues. The encapsulation of methotrexate in liposomal carriers presents a potentially beneficial strategy to enhance its therapeutic effectiveness by improving drug retention, targeting tumors more effectively, decreasing systemic toxicity, and allowing for a sustained release of the drug. The physical and chemical properties of liposomes, such as their size, polydispersity index, surface charge, and drug entrapment efficiency, are critical in influencing their stability, distribution in the body, and overall therapeutic effectiveness. Thus, systematic optimization of the formulation parameters is vital for creating an efficient liposomal drug delivery system. Employing Quality by Design (QbD) principles and statistical experimental

frameworks like the Box–Behnken Design (BBD) offers valuable methodologies for refining key formulation variables while minimizing the number of experiments and identifying interactions among those variables. In this study, liposomes containing methotrexate were created using the thin-film hydration method and were optimized through a Box–Behnken experimental design. The formulations produced were analyzed for various characteristics, including particle size, polydispersity index, zeta potential, drug content, entrapment efficiency, in vitro drug release, and solid-state properties using appropriate analytical methods. The aim of this research was to formulate an optimized liposomal system that enhances the delivery and therapeutic efficacy of methotrexate for cancer treatment, while also improving the stability of the formulation and allowing for controlled drug release.

DRUG PROFILE:

- ✓ **Drug profile: Methotrexate**
- ✓ **Generic Name:** Methotrexate
- ✓ **ChemicalName:**(2S)-2-[(4-{[(2,4-diamino-6-teridinyl)methyl]methylamino}benzoyl)amino] pentanedioic acid.
- ✓ **Molecular Formula:** $C_{29}H_{34}N_8O_{10}$
- ✓ **Molecular Weight:** 454.44 g/mol

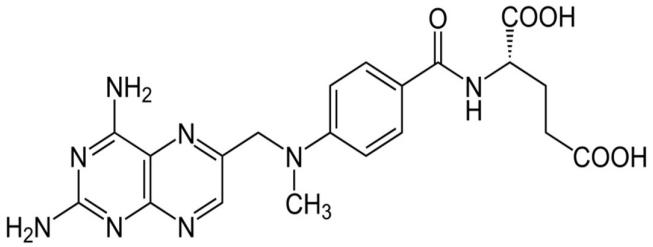

- ✓ **Drug Class:** Antimetabolite Antineoplastic agent & Disease-modifying antirheumatic drug (DMARD)

Mechanism of Action:

An analog of folic acid, methotrexate prevents the production of tetrahydrofolate by inhibitin g dihydrofolate reductase (DHFR).This inhibitor reduces cell growth by interfering with the s ynthesis of DNA, RNA, and protens.It works well in cancer treatment because its cytotoxic ef fect is most noticeable in cells that divide quickly.

Indications:

Steosarcoma, breast cancer, acute lymphoblastic leukemia, and rheumatoid arthritis (low-dose treatment) Psoriasis

Forms of Dosage:Tablets taken orally

IV/IM/subcutaneous injectable solution Pharmacokinetics:

• Absorption: ~70% oral bioavailability (decreases with higher doses)

• Distribution: Approximately 50% of it binds to plasma proteins.

• Metabolism: The liver partially converts it into active polyglutamated forms.

• Excretion: Mostly renal by tubular secretion and glomerular filtration

• Half-life: 3–10 hours for low doses, longer for high doses

Adverse Reactions:• Hepatotoxicity and myelosuppression (leukopenia, thrombocytopenia)

• Disorders of the gastrointestinal tract (nausea, vomiting, stomatitis)

Rarely, pulmonary toxicity can occur. Store at room temperature (15–

30°C). Keep out of direct sunlight and dampness.

MATERIAL & METHOD

Material:

Table no: List of Chemicals

Sr. No.	Material	Manufacturer Name	Supplied By
1	Soya lecithin	Cosmo Chem Pvt. Ltd.	Solanki Enterprises
2	Cholesterol	Cosmo Chem Pvt. Ltd.	Solanki Enterprises
3	Chloroform	Research Lab Fine Chem Industries, Mumbai	Solanki Enterprise, Pune
4	Dimethyl sulfoxide (DMSO)	Research Lab Fine Chem Industries, Mumbai	Solanki Enterprise, Pune
5	Ethanol	Research Lab Fine Chem Industries, Mumbai	Solanki Enterprise, Pune
6	Phosphate Buffer Saline (PBS, pH 7.4)	Cosmo Chem. Pvt. Ltd.	Solanki enterprises
7	Dialysis Membrane (MWCO 1000 Da)	Cosmo Chem. Pvt. Ltd.	Solanki enterprises
8	Deionized Water	Cosmo Chem. Pvt. Ltd.	Solanki enterprises
9	Methanol	Research Lab Fine Chem industries ,Mumbai	Solanki enterprise pune

Sr. No.	Instrument / Equipment Name	Company	Model Number
1.	UV-Visible spectroscopy	Jasco v-630	B206461148
2.	Centrifuge	Eltek	OC 2F
3.	Particle size, Zeta	Horiba	LA 300

Table no: List of Equipment

	Potential		
4.	FTIR	FT/IR-4600typeA	F193061786
5.	TEM	JEOL	2200FS
6.	DSC	METTLER TOLEDO, SW STARe, USA	30139230
7.	XRD	Bruker D8 Advance	D8 Advance Series 1
8.	Franz diffusion cell	DBK	210796
9.	Analytical balance	wensar	KAB2L

Methods:

Design of Experiments

A Quality by Design (QbD) approach with response surface methodology (RSM) was used to optimiz e the formulation of liposomes loaded with methotrexate.The impacts of independent variables can be methodically investigated using a Box-Behnken-design.

Hydration time, cholesterol concentration, and lipid concentration (soyalecithin) were chosen as indep endent variables.To assess their impact on the formulation's properties, they were changed at predefin ed low, medium, and high levels.Particle size (nm), polydispersity index (PDI), and entrapment efficie ncy (%) were the dependent variables (responses).

Table : List of Independent and Dependent variables in Box–Behnken design

Independent variables	Low value (-1)	High value (+)
Lipid concentration (mg)	50	100
Cholesterol concentration (mg)	5	25
Hydration time (min)	30	50
Dependent variables	Constraints Minimize Minimize	
Particle size(nm)		
Polydispersity index		
Entrapment efficiency (%)		

Table : DOE Suggested and Experimental batches

Formulation Code	Methotrexate (mg)	Soyalecithin	Cholesterol	Hydration time	Hydration medium (pH 7.4) mL
M1	30	75	15	40	20
M2	30	50	5	40	20
M3	30	75	25	30	20
M4	30	75	5	30	20
M5	30	100	15	50	20

M6	30	50	15	30	20
M7	30	75	5	50	20
M8	30	50	15	50	20
M9	30	100	5	40	20
M10	30	100	15	30	20
M11	30	50	25	40	20
M12	30	100	25	40	20
M13	30	75	25	50	20

RESULTS AND DISCUSSION

PREFORMULATION STUDY OF METHOTREXATE

Identification of drug Appearance

Active pharmaceutical ingredient: Methotrexate

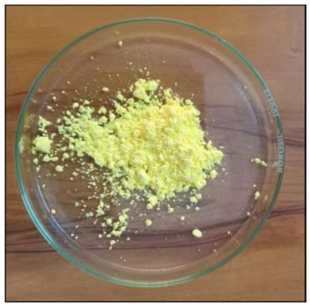

Figure 13: Methotrexate

Appearance : Crystalline powder that is yellow or pale yellow in color.

Taste: Bitter

Odour: Odorless

Solubility: Frequently soluble in organic solvents like methanol and dimethyl sulfoxide (DM SO), but only slightly soluble in water; solubility increases in alkaline

Determining the melting point:
Methotrexate was found to have a melting point of 198.5 °C, which is within the stated range of 195To205 °C.This verifies the drug sample's authenticity and purity, suggesting that the m ethotrexate received is appropriate for additional formulation research.

λmax determination of Methotrexate

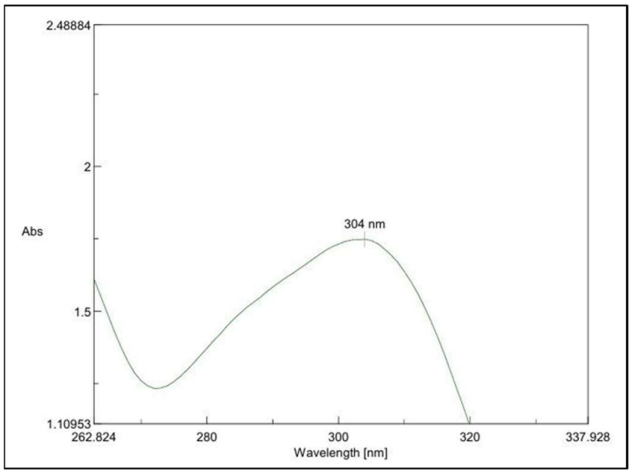

Methotrexate's observed λmax of 304 nm is within the reported range of 301–305 nm. This shows that the chosen wavelength is appropriate for additional UV spectrophotometric examination and validates the drug's identity and purity. Methotrexate's solubility

Table : Solubility study of Methotrexate in different medium

Solubility Medium	Solubility (µg/ml)	Solubility (mg/ml)
Methanol	3946.1	3.9461
Acetic Buffer 1.2	285.6	0.2856
Phosphate Buffer 6.8	2065.9	2.0659
Phosphate Buffer 7.4	2139.7	2.1397
Distilled Water	425.3	0.4253

Methotrexate's solubility research revealed that it was most soluble in methanol (3.9461 mg/ ml), followed by phosphate buffer pH 7.4 (2.1397 mg/ml) and phosphate buffer pH 6.8 (2.06 59 mg/ml)Acetic buffer pH 1.2 (0.2856 mg/ml) and distilled water (0.4253 mg/ml) showed lo wer solubility.According to these findings, methotrexate dissolves more readily in organic sol vents and slightly alkaline media than in acidic ones.

Linearity of Methotrexate

I. Calibration Curve of Methotrexate in Methanol

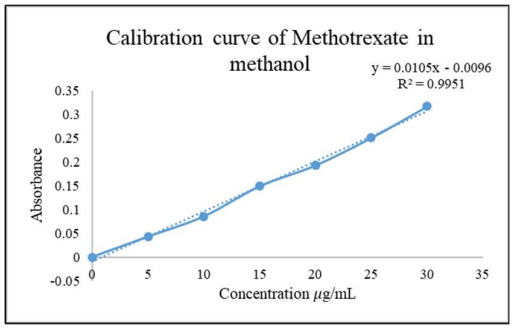

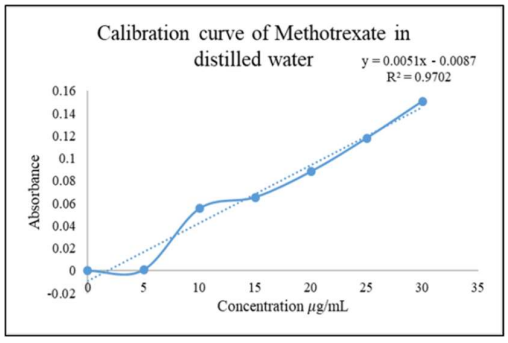

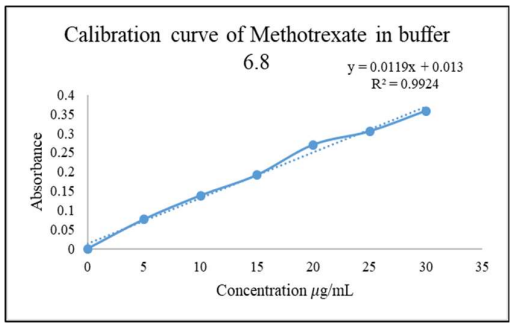

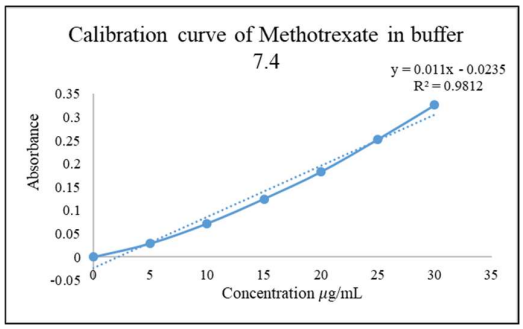

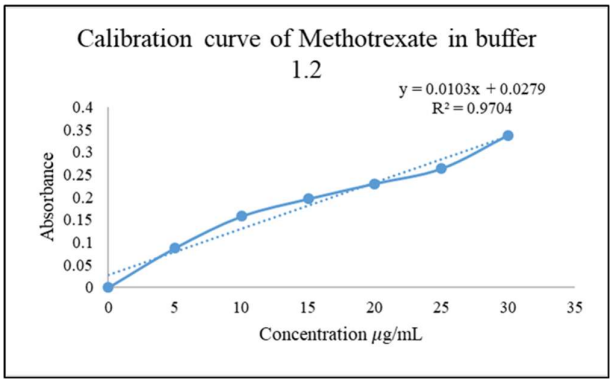

Fourier Transform Infrared Spectroscopy (FTIR)

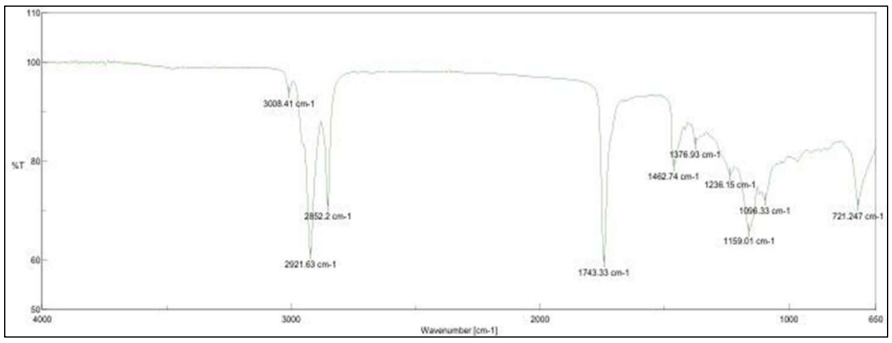

Figure : FTIR spectrum of Methotrexate

Methotrexate's FTIR spectrum verifies that its chemical structure contains distinctive functio nal groups.NH and OH stretching vibrations are represented by a large absorption band in the spectra that is located between 3200 and 3400 cm^{-1}.Aliphatic CH stretching is indicated by peaks about 2920To2850 cm^{-1}.The C=O stretching of amide and carboxylic acid groups is r epresented by a prominent absorption band around 1650To1700 cm^{-1}.The aromatic ring syste m is confirmed by the bands about 1500–1600 cm^{-1}, which show aromatic C=C stretching. Furthermore, bands between 1000 and 1150 cm^{-1} are associated with CO stretching vibration and peaks in the 1200–1300 cm^{-1} range are related to C–N stretching.

XRD

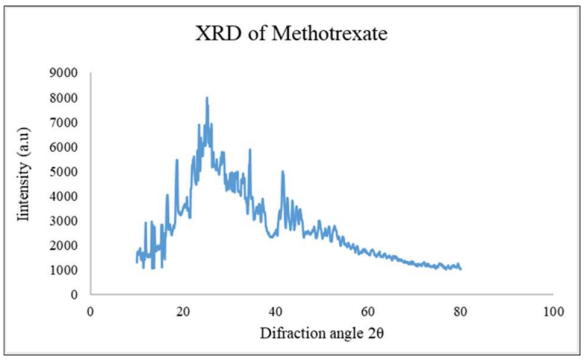

Figure 23: XRD of Methotrexate

Methotrexate Xray diffraction (XRD) pattern has multiple dense and sharp diffraction peaks i n the range of 2θ = 15–40°, which are indicative of a crystalline substance.
An organized molecular organization in the solid state is shown by the presence of distinct peaks.Overall, the XRD data show that methotrexate is present as a crystalline powder, and the observed diffraction pattern is in line with the purported crystalline nature of the medication. This attests to the sample's purity and structural integrity.

Evaluation parameters for Methotrexate loaded liposomes

Particle size, PDI and Zeta potential

Table : Particle size, PDI and Zeta potential of F1-F13

Formulation code	Particle size (nm)	PDI	Zeta potential (mV)
M1	152.4	0.243	-23.6
M2	150.8	0.203	-26.4
M3	112.5	0.125	-32.1
M4	175.6	0.277	-19.6
M5	125.3	0.169	-25.3
M6	135.4	0.178	-22.4
M7	152.3	0.237	-27.4
M8	166.5	0.263	-28.6
M9	159.4	0.308	-21.8
M10	162.3	0.322	-23.9
M11	160.6	0.266	-26.8
M12	135.6	0.243	-29.8
M13	155.9	0.309	-20.5

Particle sizes in the nanometer range (112.5To175.6 nm) were observed in the generated meth otrexateloaded liposomal formulations (M1ToM13), indicating the production of nanosized v esicles appropriate for drug delivery.The majority of formulations demonstrated satisfactory h omogeneity, and the polydispersity index (PDI) values (0.125To0.322) indicated a relatively uniform particle size distribution.The zeta potential showed sufficient surface charge and goo

d colloidal stability of the liposomal dispersions, ranging from −19.6 to −32.1 mV.With the s mallest particle size (112.5 nm), lowest PDI (0.125), and largest negative zeta potential (−32 .1 mV), M3 demonstrated the best qualities of all the formulations, indicating better stability and uniformity.As a result, M3 may offer improved stability and effective drug distribution an d can be regarded as the ideal formulation for methotrexate-loaded liposomes.

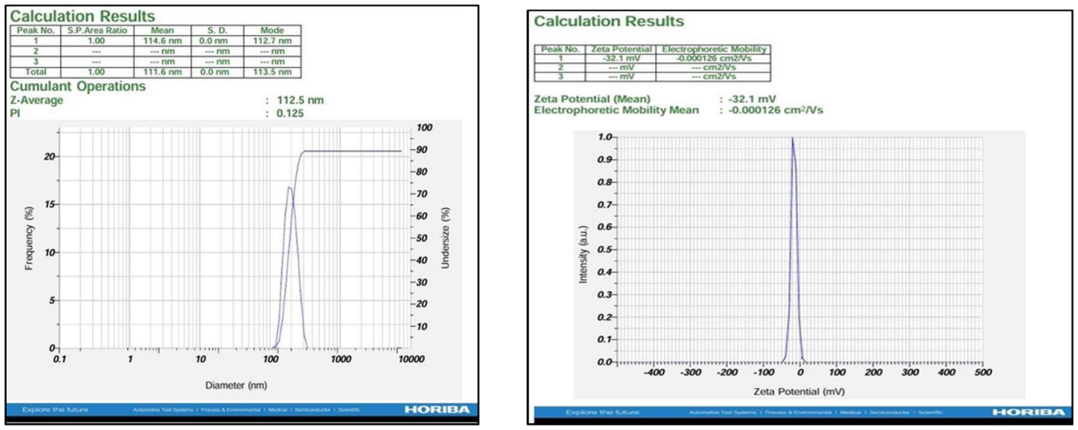

Figure : Particle size, PDI and Zeta potential graph

Table: ANOVA for 2FI model Response 1: Particle size

Source	Sum of Squares	df	Mean Square	F-value	p-value	
Model	3372.16	6	562.03	8.68	0.0094	significant
A-Lipid conc.	117.81	1	117.81	1.82	0.2261	
B-Cholesterol conc.	675.28	1	675.28	10.43	0.0179	
C-Hydration time	25.20	1	25.20	0.3892	0.5557	
AB	282.24	1	282.24	4.36	0.0819	
AC	1159.40	1	1159.40	17.90	0.0055	
BC	1112.22	1	1112.22	17.17	0.0061	
Residual	388.57	6	64.76			
Cor Total	3760.74	12				

Factor coding is coded.

Type III-Partial sum of squares: The model appears to be significant based on its F-value of 8.68.An Fvalue this large is just 0.94% likely to be the result of noise.
Model terms are consider.significant if the Pvalue is less than 0.0500.B, AC, and BC are imp ortant model terms in this instance.The model terms are not significant if the value is more th an 0.1000.Model reduction may help your model if there are a lot of unnecessary model term s (not including those needed to maintain hierarchy).

Fit Statistics

Std. Dev.	**8.05**		**R^2**	**0.8967**
Mean	149.58		Adjusted R^2	0.7934
C.V. %	5.38		Predicted R^2	0.6321
			Adeq Precision	8.7591

Coefficients in Terms of Coded Factors

Factor	Coefficient Estimate	df	Standard Error	95% CI Low	95% CI High	VIF
Intercept	149.58	1	2.23	144.12	155.05	
A-Lipid conc.	-3.84	1	2.85	-10.80	3.12	1.0000
B-Cholesterol conc.	-9.19	1	2.85	-16.15	-2.23	1.0000
C-Hydration time	1.77	1	2.85	-5.19	8.74	1.0000
AB	-8.40	1	4.02	-18.25	1.45	1.0000
AC	-17.03	1	4.02	-26.87	-7.18	1.0000
BC	16.67	1	4.02	6.83	26.52	1.0000

When all other factors are maintained constant, the coefficient estimate shows the anticipated change in reaction per unit change in factor value.
In an orthogonal design, the average reaction over all runs is called the intercept.
Depending on the factor parameters, the coefficients are modifications made to that average.
VIFs are 1 when the factors are orthogonal; VIFs larger than 1 show multicolinearity; the hig her the VIF, the more severe the factor correlation. VIFs below 10 are generally acceptable.

Final Equation in Terms of Coded Factors

Particle size	=
+149.58	
-3.84	A
-9.19	B
+1.77	C
-8.40	AB
-17.03	AC
+16.67	BC

Predictions regarding the response for specific amounts of each element can be made using the equation in terms of coded factors.By default, the factors' high and low levels are coded a s +1 and 1, respectively.By comparing the factor coefficients, the coded equation can be used to determine the relative impact of the components.

Final Equation in Terms of Actual Factors

Particle size	=
+25.72837	
+3.07450	Lipid conc.
-5.06875	Cholesterol conc.
+2.78375	Hydration time
-0.033600	Lipid conc. * Cholesterol conc.
-0.068100	Lipid conc. * Hydration time
+0.166750	Cholesterol conc. * Hydration time

Predictions regarding the reaction for specific levels of each element can be made using the e quation in terms of actual factors.In this case, each factor's levels should be given in its origin al units.Because the intercept is not in the middle of the design space and the coefficients are scaled to account for the units of each element, this equation should not be used to calculate t he relative influence of each factor.

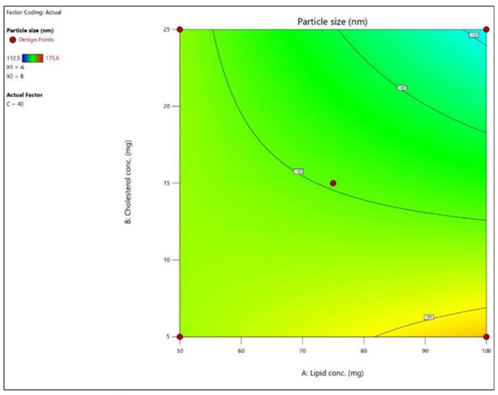

Figure : Contour plot for particle size

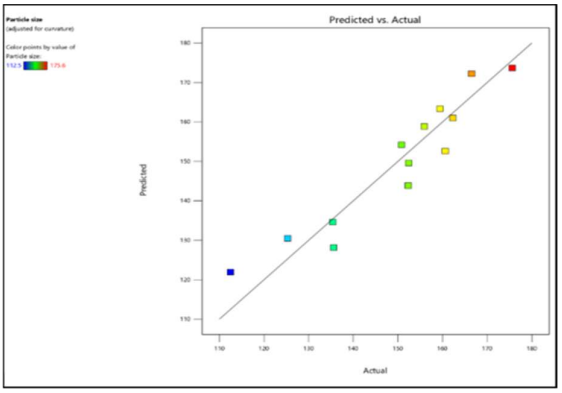

Figure : Predicted vs actual plot forparticle size

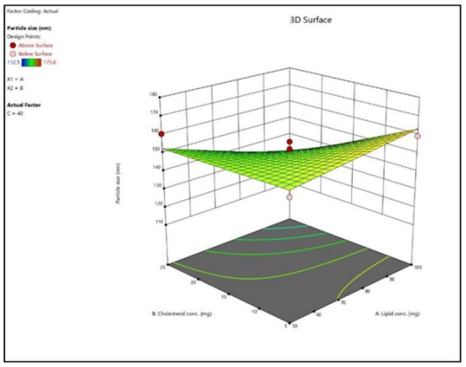

Figure : 3D Surface plot for particle size

ANOVA for 2FI model Response 2: Polydispersity index

Source	Sum of Squares	df	Mean Square	F-value	p-value	
Model	0.0345	6	0.0058	4.54	0.0440	significant
A-Lipid conc.	0.0022	1	0.0022	1.72	0.2379	
B-Cholesterol conc.	0.0008	1	0.0008	0.6630	0.4466	
C-Hydration time	0.0007	1	0.0007	0.5695	0.4790	
AB	0.0041	1	0.0041	3.23	0.1224	
AC	0.0142	1	0.0142	11.17	0.0156	
BC	0.0125	1	0.0125	9.89	0.0199	
Residual	0.0076	6	0.0013			
Cor Total	0.0421	12				

Factor coding is coded.

Type III-Partial sum of squares The model's significance is indicated by its F-value of 4.54. An Fvalue this high is only 4.40% likely to be caused by noise.Model terms are considered si gnificant if the Pvalue is less than 0.0500.AC and BC are important model terms in this instan ce.The model terms are not significant if the value is more than 0.1000.Model reduction may help your model if there are a lot of unnecessary model terms (not including those needed to maintain hierarchy).

Fit Statistics

Std. Dev.	0.0356	R^2	0.8195
Mean	0.2418	Adjusted R^2	0.6390
C.V. %	14.73	Predicted R^2	0.5481
		Adeq Precision	5.8176

Coefficients in Terms of Coded Factors

Factor	Coefficient Estimate	df	Standard Error	95% CI Low	95% CI High	VIF
Intercept	0.2418	1	0.0099	0.2176	0.2659	
A-Lipid conc.	0.0165	1	0.0126	-0.0143	0.0473	1.0000
B-Cholesterol conc.	-0.0103	1	0.0126	-0.0411	0.0206	1.0000
C-Hydration time	0.0095	1	0.0126	-0.0213	0.0403	1.0000
AB	-0.0320	1	0.0178	-0.0756	0.0116	1.0000
AC	-0.0595	1	0.0178	-0.1031	-0.0159	1.0000
BC	0.0560	1	0.0178	0.0124	0.0996	1.0000

When all other factors are maintained constant, the coefficient estimate shows the anticipated change in reaction per unit change in factor value.In an orthogonal design, the average reactio n over all runs is called the intercept.Depending on the factor parameters, the coefficients are modifications made to that average.VIFs are 1 when the factors are orthogonal; VIFs larger th

an 1 show multicolinearity; the higher the VIF, the more severe the factor correlation.VIFs be low 10 are generally considered acceptable.

Final Equation in Terms of Coded Factors

Polydispersity index	=
+0.2418	
+0.0165	A
-0.0103	B
+0.0095	C
-0.0320	AB
-0.0595	AC
+0.0560	BC

Predictions regarding the response for specific amounts of each element can be made using th e equation in terms of coded factors.By default, the factors' high and low levels are coded as +1 and 1, respectively.By comparing the factor coefficients, the coded equation can be used t o determine the relative impact of the components.

Final Equation in Terms of Actual Factors

Polydispersity index	=
-0.352356	
+0.012100	Lipid conc.
-0.013825	Cholesterol conc.
+0.010400	Hydration time
-0.000128	Lipid conc. * Cholesterol conc.
-0.000238	Lipid conc. * Hydration time
+0.000560	Cholesterol conc. * Hydration time

Predictions regarding the reaction for specific levels of each element can be made using the e quation in terms of actual factors.In this case, each factor's levels should be given in its origin al units.Because the intercept is not in the middle of the design space and the coefficients are scaled to account for the units of each element, this equation should not be used to calculate t he relative influence of each factor.

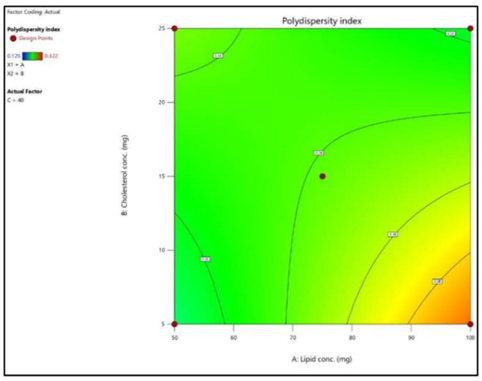

Figure : Contour plot for PDI

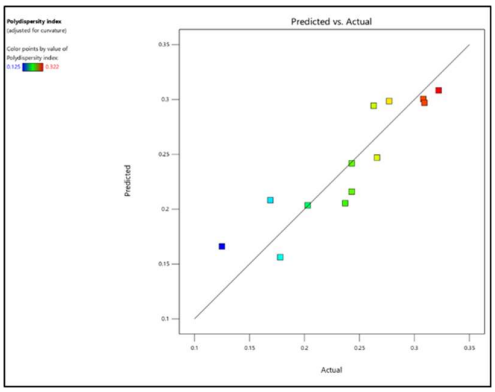

Figure : Predicted vs actual plot for PDI

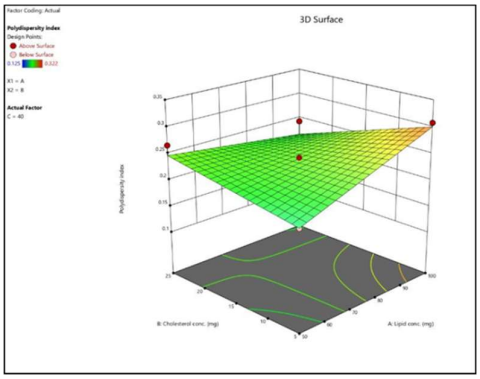

Figure : 3D Surface plot for PDI

Morphology study by TEM

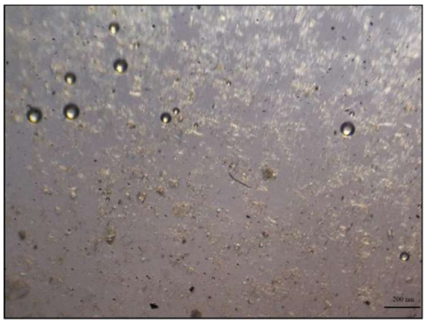

Figure : TEM of optimized batch M3

The optimized batch M3's TEM picture demonstrates the development of uniformly shaped, widely dispersed nanoparticles.As is frequently seen in nanoparticulate systems, the particles appear almost spherical with minor aggregation in some areas.

The particle dispersion shows that stable, distinct nanoparticles were effectively created durin g the formulation process.Overall, the TEM results indicate the modified formulation's (M3)

appropriateness for improved drug delivery performance by confirming the nanoscale particle production and good dispersion.

Drug content

Table : % Drug content of M1-M13

Formulation code	Drug content (%)
M1	91.56±0.002
M2	84.56±0.001
M3	95.62±0.002
M4	88.46±0.002
M5	93.26±0.003
M6	89.16±0.004
M7	85.62±0.001
M8	87.19±0.004
M9	92.87±0.003
M10	86.45±0.002
M11	90.26±0.001
M12	84.88±0.002
M13	91.68±0.001

Methotrexateloaded liposomal formulations (M1ToM13) had drug contents ranging from 84. 56% to 95.62%, suggesting that the drug was satisfactorily incorporated into the liposomal ve sicles.The majority of formulations had drug contents more than 85%, indicating effective dr ug loading and little drug loss during preparation.M3 had the highest drug content (95.62%) o f all the batches, suggesting that it was more effective at entraping drugs than the other formu lations.Based on its highest drug concentration and superior formulation properties, M3 was d etermined to be the most appropriate formulation. The results verify that the liposomal formul ations were effectively created with good drug loading capacity.

Entrapment efficiency

Table : % Entrapment efficiency of M1-M13

Formulation code	Entrapment efficiency (%)
M1	80.23±0.003
M2	76.48±0.002
M3	87.45±0.002
M4	78.36±0.004
M5	83.16±0.001
M6	74.86±0.001
M7	77.94±0.001
M8	80.15±0.002
M9	83.46±0.002

M10	82.54±0.001
M11	79.96±0.004
M12	84.12±0.004
M13	82.16±0.004

Methotrexateloaded liposomal formulations (M1M13) had entrapment efficiencies ranging fr om 74.86% to 87.45%, demonstrating the drug's successful integration into the liposomal vesi cles.The majority of formulations had entrapment efficiency above 75%, indicating the liposo mal system's strong drug loading capacity.M3 demonstrated the highest entrapment efficiency (87.45%) of all batches, indicating superior drug encapsulation and stability in comparison to other formulations.These findings show that the liposomal formulations were successfully m ade with acceptable entrapment efficiency, and M3 was found to be the best formulation beca use of its better drug loading capabilities**.**

ANOVA for Linear model Response 3: Entrapment efficiency

Source	Sum of Squares	df	Mean Square	F-value	p-value	
Model	97.64	3	32.55	6.56	0.0121	significant
A-Lipid conc.	59.57	1	59.57	12.01	0.0071	
B-Cholesterol conc.	38.06	1	38.06	7.67	0.0218	
C-Hydration time	0.0050	1	0.0050	0.0010	0.9754	
Residual	44.65	9	4.96			
Cor Total	142.28	12				

Factor coding is coded.

Type III-Partial sum of squares

The model is considered significant based on its Fvalue of 6.56.An Fvalue this high has a 1.2 1% probability of being caused by noise.Model terms are considered significant if the Pvalue is less than 0.0500.A and B are important model terms in this instance.The model terms are n ot significant if the value is more than 0.1000.Model reduction may help your model if there are a lot of unnecessary model terms (not including those needed to maintain hierarchy).

Fit Statistics

Std. Dev.	2.23	R^2	0.6862
Mean	80.84	Adjusted R^2	0.5816
C.V. %	2.76	Predicted R^2	0.4100
		Adeq Precision	7.9485

Coefficients in Terms of Coded Factors

Factor	Coefficient Estimate	df	Standard Error	95% CI Low	95% CI High	VIF
Intercept	80.84	1	0.6177	79.44	82.23	
A-Lipid conc.	2.73	1	0.7875	0.9474	4.51	1.0000
B-Cholesterol conc.	2.18	1	0.7875	0.3999	3.96	1.0000
C-Hydration time	0.0250	1	0.7875	-1.76	1.81	1.0000

When all other factors are maintained constant, the coefficient estimate shows the anticipated change in reaction per unit change in factor value.In an orthogonal design, the average reactio n over all runs is called the intercept.Depending on the factor parameters, the coefficients are modifications made to that average.VIFs are 1 when the factors are orthogonal; VIFs larger th an 1 show multicolinearity; the higher the VIF, the more severe the factor correlation.VIFs be low 10 are generally considered acceptable.

Final Equation in Terms of Coded Factors

Entrapment efficiency	=
+80.84	
+2.73	A
+2.18	B
+0.0250	C

Predictions regarding the response for specific amounts of each element can be made using th e equation in terms of coded factors.By default, the factors' high and low levels are coded as +1 and 1, respectively.By comparing the factor coefficients, the coded equation can be used t o determine the relative impact of the components.

Final Equation in Terms of Actual Factors

Entrapment efficiency	=
+69.27803	
+0.109150	Lipid conc.
+0.218125	Cholesterol conc.
+0.002500	Hydration time

Predictions regarding the reaction for specific levels of each element can be made using the e quation in terms of actual factors.In this case, each factor's levels should be given in its origin

al units.Because the intercept is not in the middle of the design space and the coefficients are scaled to account for the units of each element, this equation should not be used to calculate t he relative influence of each factor.

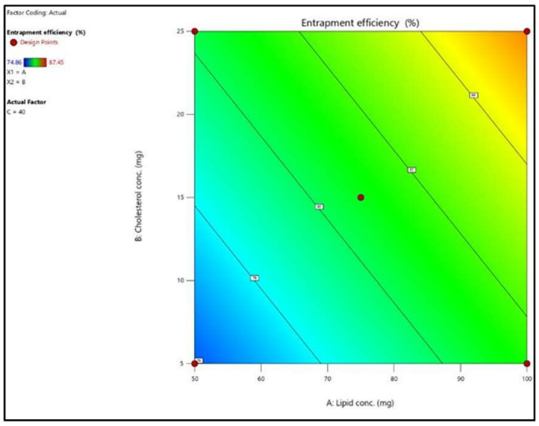

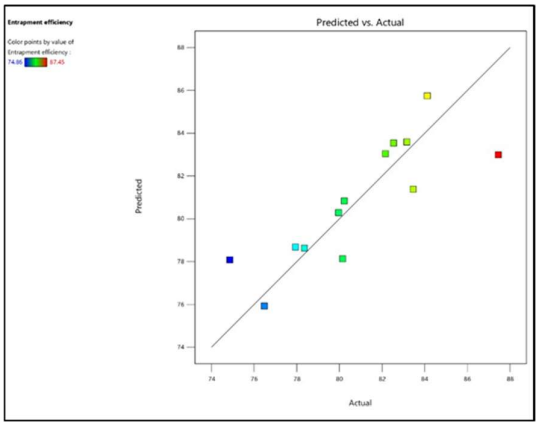

Figure : Contour plot for entrapment efficiency Figure : Predicted vs actual plot for entrapment efficiency

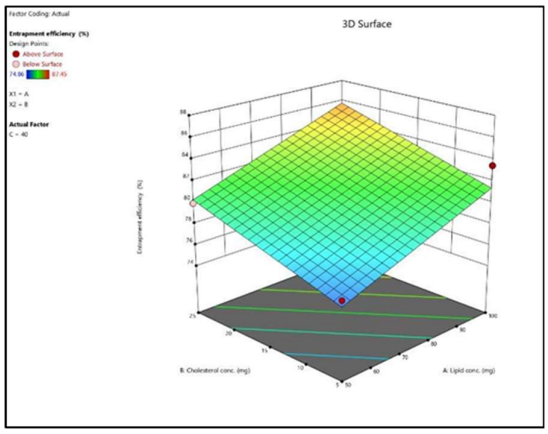

Figure : 3D surface plot for entrapment efficiency

In vitro drug release study

Table : In vitro drug release of M1-M7

Time (Hr)	M1	M2	M3	M4	M5	M6	M7
0	0	0	0	0	0	0	0
0.5	9.13±0.001	9.58±0.004	11.57±0.002	7.54±0.004	10.45±0.004	16.17±0.003	8.40±0.002
1	13.02±0.004	16.02±0.003	18.23±0.004	12.14±0.002	14.16±0.002	19.63±0.004	15.77±0.001
2	18.98±0.0	23.49±0.0	23.03±0.0	18.98±0.0	20.94±0.0	25.68±0.0	27.33±0.0

	03	02	01	01	04	03	03
4	22.48±0.002	30.28±0.002	50.01±0.004	27.41±0.004	26.57±0.001	38.00±0.001	36.95±0.001
6	28.61±0.004	44.17±0.003	56.36±0.002	44.87±0.002	42.76±0.003	49.08±0.004	49.64±0.004
8	45.62±0.002	58.60±0.004	63.26±0.004	52.39±0.004	61.53±0.004	57.79±0.002	61.71±0.002
12	65.62±0.001	72.56±0.003	80.01±0.003	66.58±0.001	75.08±0.003	68.69±0.004	71.14±0.003
24	75.87±0.003	79.19±0.001	92.88±0.001	76.65±0.002	84.06±0.004	86.03±0.004	83.50±0.004

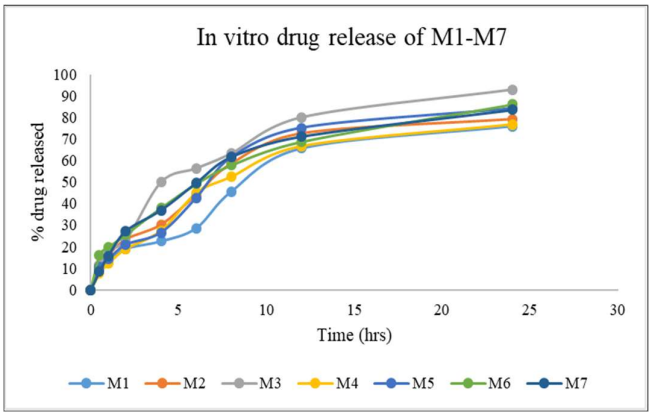

Figure : In vitro drug release of M1-M7

Table : In vitro drug release of M8-M13

Time (Hr)	M8	M9	M10	M11	M12	M13
0	0	0	0	0	0	0
0.5	8.20±0.002	9.6±0.004	9.57±0.001	17.36±0.002	9.39±0.002	16.17±0.001
1	17.41±0.003	18.88±0.003	18.40±0.001	23.07±0.003	16.95±0.004	25.54±0.002
2	27.33±0.001	32.20±0.001	32.87±0.002	34.91±0.004	22.90±0.002	31.78±0.003
4	36.13±0.004	41.44±0.002	38.48±0.003	45.15±0.002	31.18±0.004	37.87±0.004
6	49.61±0.003	52.26±0.004	53.03±0.002	52.51±0.003	45.20±0.004	43.37±0.003
8	57.67±0.004	64.42±0.002	62.58±0.001	66.64±0.004	59.34±0.002	59.94±0.002
12	63.39±0.002	72.62±0.003	72.20±0.004	77.90±0.003	73.29±0.003	80.54±0.001
24	75.46±0.003	82.93±0.004	84.69±0.003	90.92±0.004	78.74±0.002	89.94±0.004

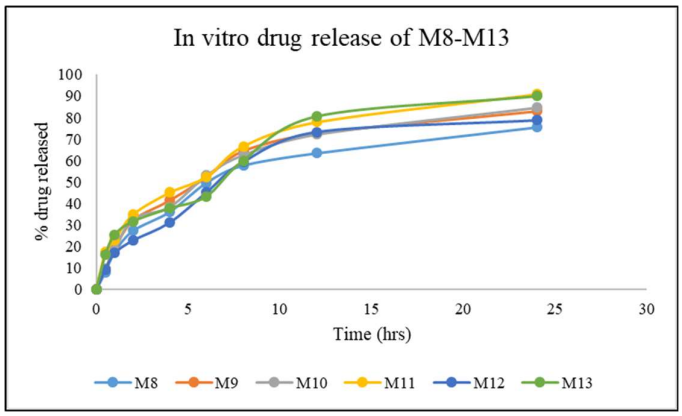

Figure In vitro drug release of M8-M13

Drug release gradually increases over a period of up to 24 hours, according to the in-vitro drug release research of several formulations (M1M13).M3 showed the highest cumulative drug release (92.88%) at 24 hours among all formulations, suggesting superior drug dispersion and release properties in comparison to other batches.Although they were somewhat less than M3, other formulations like M11 (90.93%) and M13 (89.94%) also displayed comparatively high drug release.For controlled drug delivery systems, the release profile of the majority of formulations shows an initial burst release followed by a sustained drug release pattern.Because of its maximum and continuous drug release over a 24hour period, formulation M3 was determined to be the optimal formulation based on the cumulative percentage drug release and overall release behavior.

FTIR

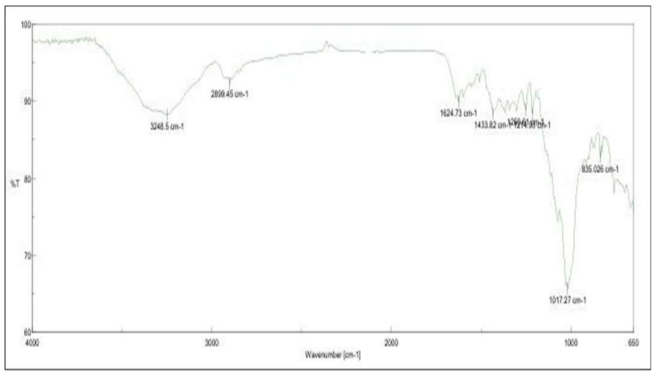

Figure : FTIR spectrum of optimized batch M3

The existence of the medication and lipid components in the formulation is confirmed by the FTIR spectrum of optimized liposomal batch M3, which displays distinctive absorption peaks . O–H/N–H stretching vibrations are represented by the large peak at 3248.5 cm^{-1}. C–H stretching of aliphatic lipid chains is seen by the signal at 2889.45 cm^{-1}.

C=C or amide stretching vibrations are represented by a band at 1624.73 cm^{-1}.
The peak at 1433.82 cm^{-1} corresponds to CH_2 bending of fatty acid chains in phospholipids.
The phospholipid ester group's P–O–C stretching is seen by the band at 1017.27 cm^{-1}. C-H bending vibrations could be the cause of the peak at 835.02 cm^{-1}.

XRD

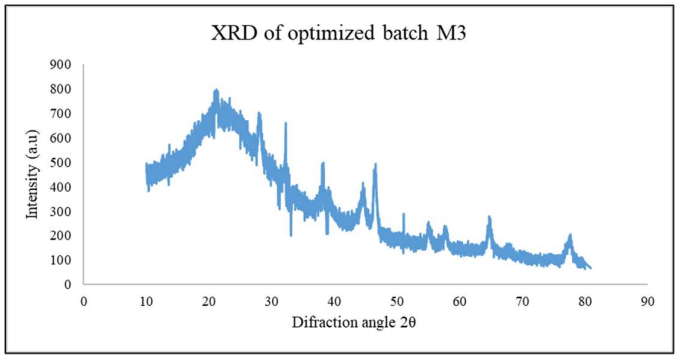

Figure : XRD of optimized batch M3

The optimized batch M3's XRD pattern reveals a wide hump with a few low-intensity peaks, suggesting that the encapsulated medication is primarily amorphous.
The drug may be molecularly distributed within the liposomal matrix if there are no distinct, high-intensity crystalline peaks.
The prolonged and better release seen in the in vitro trials may be attributed to this amorphization's ability to increase drug solubility and dissolution rate.
Overall, the XRD data show that the medication was successfully encapsulated in a mostly amorphous state, which is advantageous for increased bioavailability.

Stability study

Table : Stability study of optimized batch M3

Months	Parameters		
	Particle size (nm)	PDI	Entrapment efficiency (%)
0	112.5	0.125	87.45
1	112.8	0.126	87.32
2	113.6	0.126	86.15
3	115.4	0.128	85.96

The optimized formulation maintained its physical and chemical stability for three months, according to the stability study results.Particle aggregation was low, as evidenced by only minor increases in particle size (112.5–115.4 nm) and PDI (0.125–0.128).
From 87.45% to 85.96%, the entrapment efficiency decreased very slightly, indicating minimal drug leakage during storage.The optimized formulation is stable during the storage period, as evidenced by the formulation's overall good stability and lack of notable changes in particle size, polydispersity index, or entrapment efficiency.

Summary

In order to enhance medication targeting, lower toxicity, and accomplish controlled drug relea se, this work concentrated on creating and refining a methotrexate-loaded liposomal drug delivery system for anticancer therapy.Methotrexate's purity, compatib ility, and crystalline nature were validated by preformulation experiments. The thin film hydration process was used to prepare liposomes, which were then optimized using a BoxBehnken design.With the smallest particle size (112.5 nm), low PDI (0.125), high zeta po tential (−32.1 mV), maximum entrapment efficiency (87.45%), and highest cumulative drug r elease (92.88% over 24 hours), M3 outperformed the other 13 formulations.While FTIR and XRD tests showed drugexcipient compatibility and effective drug encapsulation, TEM verifie d spherical, welldispersed liposomes.Threemonth stability tests revealed no variation in the fo rmulation's characteristics, suggesting strong chemical and physical stability.
All things considered, the improved liposomal formulation showed encouraging promise as a stable and efficient controlled drug delivery method for methotrexate in cancer treatment.

CONCLUSION
Methotrexateloaded liposomes for anticancer therapy were successfully created and optimize d in this work.Preformulation investigations verified methotrexate's authenticity, purity, and a ppropriate physicochemical characteristics.Soy lecithin and cholesterol were used in the thin f ilm hydration process to create liposomes.Nanosized particles with adequate PDI, zeta potenti al, drug content, and entrapment efficiency were present in all formulations.M3 demonstrated the best properties of all the formulations, including reduced particle size, increased entrapm ent effectiveness, and enhanced drug release.The drug's amorphous dispersion and drugexcipi ent compatibility were validated by FTIR and XRD analysis, while the in vitro drug release in vestigation demonstrated sustained release up to 24 hours.According to stability experiments, the optimized formulation did not change while being stored.
Overall, the modified liposomal formulation showed substantial drug loading, sustained drug release, and good stability, indicating that it may be a useful drug delivery method for antican cer treatment.

REFERENCES

1. Raina S, Sharma V, Kour N, Sharma S. INCREASED RISK OF DIFFERENT TYPES OF CANCERS IN THE STATE OF JAMMU AND KASHMIR: A COMPREHENSIVE REVIEW. World Journal of Pharmacy and Pharmaceutical Sciences. 2019 Feb 20;8(4):1427-36.
2. Noble CO, Guo Z, Hayes ME, Marks JD, Park JW, Benz CC, Kirpotin DB, Drummond DC. Characterization of highly stable liposomal and immunoliposomal formulations of vincristine and vinblastine. Cancer chemotherapy and pharmacology. 2009 Sep;64(4):741- 51
3. Fernald K, Kurokawa M. Evading apoptosis in cancer. Trends in cell biology. 2013 Dec 1;23(12):620-33.
4. Narayanan DL, Saladi RN, Fox JL. Ultraviolet radiation and skin cancer. International journal of dermatology. 2010 Sep;49(9):978-86.
5. IARC Working Group on the Evaluation of Carcinogenic Risks to Humans, International Agency for Research on Cancer. Biological agents. IARC Monogr Eval Carcinog Risks Hum. 2012;100:1.
6. Martin D, Gutkind JS. Human tumor-associated viruses and new insights into the molecular mechanisms of cancer. Oncogene. 2008 Dec;27(2):S31-42.
7. van Elsland D, Neefjes J. Bacterial infections and cancer. The EMBO Reports. 2018 Nov 1;19(11):EMBR201846632.
8. Reuter S, Gupta SC, Chaturvedi MM, Aggarwal BB. Oxidative stress, inflammation, and cancer: Free radical biology and medicine. 2010 Dec 1;49(11):1603-16.
9. Bansal V, Kim KH. Review of PAH contamination in food products and their health hazards. Environment international. 2015 Nov 1;84:26-38.
10. Puangsombat K, Gadgil P, Houser TA, Hunt MC, Smith JS. Occurrence of heterocyclic amines in cooked meat products. Meat science. 2012 Mar 1;90(3):739-46.
11. Praud D, Rota M, Rehm J, Shield K, Zatoński W, Hashibe M, La Vecchia C, Boffetta P. Cancer incidence and mortality attributable to alcohol consumption. International journal of cancer. 2016 Mar 15;138(6):1380-7.
12. Vishnu BV, Raosaheb KV. Formulation and Evaluation of Liposomes from Vinca Flowers Extract for Anti Cancer.

13. Hanahan D, Weinberg RA. Hallmarks of cancer: the next generation. cell. 2011 Mar 4;144(5):646-74.

14. Osler W. The principles and practice of medicine. D. Appleton and Company; 1912.

15. JH B. Edwin Smith surgical papyrus. Facsimile and Hieroglyphic Transliteration with Translation and Commentary. 1930;2.

16. Ghaemi B, Mashinchian O, Mousavi T, Karimi R, Kharrazi S, Amani A. Harnessing the cancer radiation therapy by lanthanide-doped zinc oxide based theranostic nanoparticles. ACS applied materials & interfaces. 2016 Feb 10;8(5):3123-34.

17. Silk AW, Margolin K. Cytokine therapy. Hematology/Oncology Clinics. 2019 Apr 1;33(2):261-74.

18. Farkona S, Diamandis EP, Blasutig IM. Cancer immunotherapy: the beginning of the end of cancer?. BMC medicine. 2016 May 5;14(1):73.

19. Shevtsov M, Sato H, Multhoff G, Shibata A. Novel approaches to improve the efficacy of immuno-radiotherapy. Frontiers in oncology. 2019 Mar 19;9:156.

20. Rodríguez-Ruiz ME, Vanpouille-Box C, Melero I, Formenti SC, Demaria S. Immunological mechanisms responsible for radiation-induced abscopal effect. Trends in immunology. 2018 Aug 1;39(8):644-55.

21. Chen J, Fan T, Xie Z, Zeng Q, Xue P, Zheng T, Chen Y, Luo X, Zhang H. Advances in nanomaterials for photodynamic therapy applications: Status and challenges. Biomaterials. 2020 Apr 1;237:119827.

22. Yang L, DeBusk LM, Fukuda K, Fingleton B, Green-Jarvis B, Shyr Y, Matrisian LM, Carbone DP, Lin PC. Expansion of myeloid immune suppressor Gr+ CD11b+ cells in tumor-bearing host directly promotes tumor angiogenesis. Cancer cell. 2004 Oct 1;6(4):409-21.

23. Zaorsky NG, Harrison AS, Trabulsi EJ, Gomella LG, Showalter TN, Hurwitz MD, Dicker AP, Den RB. Evolution of advanced technologies in prostate cancer radiotherapy. Nature Reviews Urology. 2013 Oct;10(10):565-79.

24. Hu M, Jiang L, Cui X, Zhang J, Yu J. Proton beam therapy for cancer in the era of precision medicine. Journal of hematology & oncology. 2018 Dec 12;11(1):136.

25. Decker WK, da Silva RF, Sanabria MH, Angelo LS, Guimarães F, Burt BM, Kheradmand F, Paust S. Cancer immunotherapy: historical perspective of a clinical revolution and emerging preclinical animal models. Frontiers in immunology. 2017 Aug 2;8:829.

26. Wu X, Gu Z, Chen Y, Chen B, Chen W, Weng L, Liu X. Application of PD-1 blockade in cancer immunotherapy. Computational and structural biotechnology journal. 2019 Jan 1;17:661-74.

27. Nikanjam M, Kato S, Kurzrock R. Liquid biopsy: current technology and clinical applications. Journal of hematology & oncology. 2022 Sep 12;15(1):131.

28. Jacome AA, Johnson B. Minimal residual disease in colorectal cancer: are we finding the needle in a haystack?. Cells. 2023 Apr 1;12(7):1068.

29. Riggio AI, Varley KE, Welm AL. The lingering mysteries of metastatic recurrence in breast cancer. British journal of cancer. 2021 Jan 5;124(1):13-26.

30. Tohme S, Simmons RL, Tsung A. Surgery for cancer: a trigger for metastases. Cancer research. 2017 Apr 1;77(7):1548-52.

31. Tohme S, Simmons RL, Tsung A. Surgery for cancer: a trigger for metastases. Cancer research. 2017 Apr 1;77(7):1548-52.